

Controlling a complex system near its critical point via temporal correlations

Dante R. Chialvo,^{1,2} Sergio A. Cannas,^{2,3} Dietmar Plenz,⁴ and Tomás S. Grigera^{2,5,6}

¹Center for Complex Systems & Brain Sciences (CEMSC³),

Escuela de Ciencia y Tecnología. Universidad Nacional de San Martín, San Martín, (1650) Buenos Aires, Argentina

²Consejo Nacional de Investigaciones Científicas y Tecnológicas (CONICET), Godoy Cruz 2290, Buenos Aires, Argentina

³Instituto de Física Enrique Gaviola (IFEG-CONICET),

Facultad de Matemática, Astronomía, Física y Computación,

Universidad Nacional de Córdoba, (5000) Córdoba, Argentina

⁴Section on Critical Brain Dynamics, National Institute of Mental Health, Bethesda, MD (20892), USA

⁵Instituto de Física de Líquidos y Sistemas Biológicos (IFLySiB-CONICET),

Universidad Nacional de La Plata, (1900) La Plata, Buenos Aires, Argentina

⁶Departamento de Física, Facultad de Ciencias Exactas, Universidad Nacional de La Plata, Argentina

A wide variety of complex systems exhibit large fluctuations both in space and time that often can be attributed to the presence of some kind of critical phenomena. Under such critical scenario it is well known that the properties of the correlation functions in space and time are two sides of the same coin. Here we test whether systems exhibiting a phase transition could self-tune to its critical point taking advantage of such correlation properties. We describe results in three models: the 2D Ising ferromagnetic model, the 3D Vicsek flocking model and a small-world neuronal network model. We illustrate how the feedback of the autocorrelation function of the order parameter fluctuations is able to shift the system towards its critical point. Since the results rely on universal properties they are expected to be relevant to a variety of other settings.

The last decade has witnessed an escalating interest in complex biological phenomena at all levels including macroevolution, neuroscience at different scales, and molecular biology. The observed complexity in nature is often traced to critical phenomena because it resembles the complexity found for critical dynamics in models and theory [1–8]. More specifically, it seems that many biological systems reach a “sweet spot” where they attain maximal susceptibility, i.e., sensitivity to changes in the environment, while maintaining internal order.

At present it is not clear how such a critical state can be reached or even maintained. For a complex system like the brain, one might imagine that its control parameters be hard-wired genetically, selected by a long evolutionary process to at a critical point that is biologically most advantageous for survival. However, the critical values of the control parameters *depend on system size* [9], and thus for biological systems to take advantage of critical dynamics they would need to adjust the control parameter as systems contract or expand. We exemplify this problem in Fig. 1 (inset) which sketches how the peak of the susceptibility, the property to be maximized, shifts as the system get larger.

While some physical systems might be large enough that one can assume they are asymptotically near the thermodynamic limit, we note that most biological systems are of moderate size, and finite-size effects are in principle to be expected [10]. Hence, if the critical point is the best (or only) functioning state for a given biological system, in order to attain it, Darwinian evolution instead of furnishing a set of specific values for the control parameter must allow for a *control mechanism* such that systems can reach and stay close to a critical point.

For a control mechanism to be biologically plausible it should utilize only information that either is completely global or completely local. Here we explore a possibility for such a mechanism.

We show that the first autocorrelation coefficient $AC(1)$ of the order parameter fluctuations can be used to tune a system to the vicinity of its critical point. This is possible because $AC(1)$ peaks at the same point as the susceptibility, yet does so more smoothly than the susceptibility.

This can be understood from dynamic scaling. The dynamic scaling form of the time correlation is [11]

$$C(k, t) = C_0(k)g\left(\frac{t}{\tau_0(k, \xi)}; k\xi\right), \quad (1)$$

where k is the observation wavevector, ξ is the correlation length, the function g is such that $g(t=0) = 1$, i.e. $C_0(k)$ is the static correlation function, and the characteristic time obeys

$$\tau_0(k, \xi) = k^{-z}\Gamma(k\xi; \xi/L) = \xi^z\Omega(k\xi), \quad (2)$$

where g , Γ and Ω are unspecified scaling functions and z is the dynamic scaling exponent. Now

$$\begin{aligned} \frac{C(k, t = \delta t)}{C(k, 0)} &\approx 1 + \delta t \frac{1}{C_0(k)} \frac{dC(k, t = 0)}{dt} \\ &= 1 + \delta t \xi^{-z} \Omega^{-1}(k\xi) g'(0; k\xi). \end{aligned} \quad (3)$$

For a global quantity, $k = 0$ (See Supplementary Material) so that

$$\frac{C(k = 0, \delta t)}{C(k = 0, t = 0)} \sim 1 - A \xi^{-z} \sim 1 - A(T - T_c)^{z\nu}, \quad (4)$$

where $A > 0$ is a time dependent constant. Hence, the normalized time correlation has a maximum at $T = T_c$, for fixed δt .

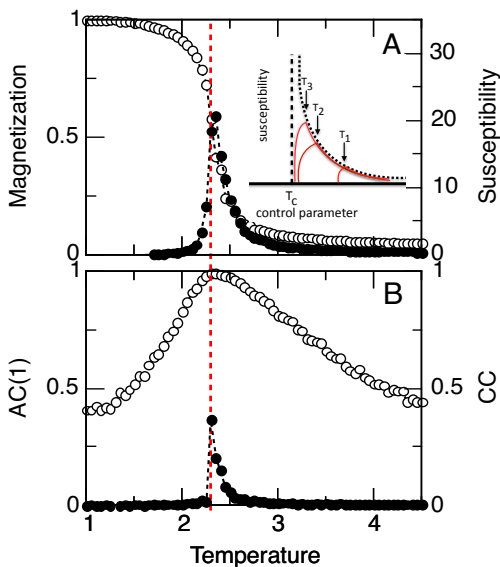


FIG. 1. Autocorrelation peaks with susceptibility at T_c in the equilibrium Ising model. Panel A: The order parameter (magnetization; open circles) and susceptibility (filled circles) as function of temperature T . Panel B: Corresponding average pairwise correlation (CC ; filled circles) and first autocorrelation coefficient ($AC(1)$; open circles) of the magnetization fluctuations around the instantaneous mean. Dashed vertical line denotes T_c . (System size $N = 32^2$, 10^4 MC steps). The inset shows a cartoon of the expected susceptibility as a function of the control parameter for three systems of increasing sizes, where arrows indicate the corresponding optimal points T_1, T_2, T_3 .

The main idea is demonstrated here by applying it to three well understood systems, namely the ferromagnetic Ising model, the Vicsek model of flocking and a typical neuronal small-world network. We remark that the results are general enough to be also expected in many other systems.

Ising model. Fig. 1 illustrates the typical behaviour of the 2D ferromagnetic Ising model at increasing temperatures. The system undergoes a second order phase transition at a critical temperature T_c , reflected in a steep change in magnetization as well as a sharp peak in susceptibility (Fig. 1A). Equally distinct changes are also demonstrated for the correlation properties of the model computed from appropriate system variables (Fig. 1B). A sharp increase in the average pairwise correlations is observed as the system approaches T_c , where the correlation length matches the size of the system. The relatively sharp changes in the spatial correlations contrast with the relatively smoother changes in the temporal correlations, as reflected by the first auto-correlation coefficient $AC(1)$ of the magnetization fluctuations around

the mean, which at T_c approaches unity.

Now we assess how to control the Ising model to stay at the vicinity of the susceptibility peak. According with the discussion in the introduction, we must restrict ourselves to do it using only either local or global information. In that sense, the time correlations evaluated by $AC(1)$ meet such conditions, because it can be computed from a temporally delayed version of a global average of magnetization. In turn, magnetization can be assessed simply by averaging samples of a relatively large number of sites.

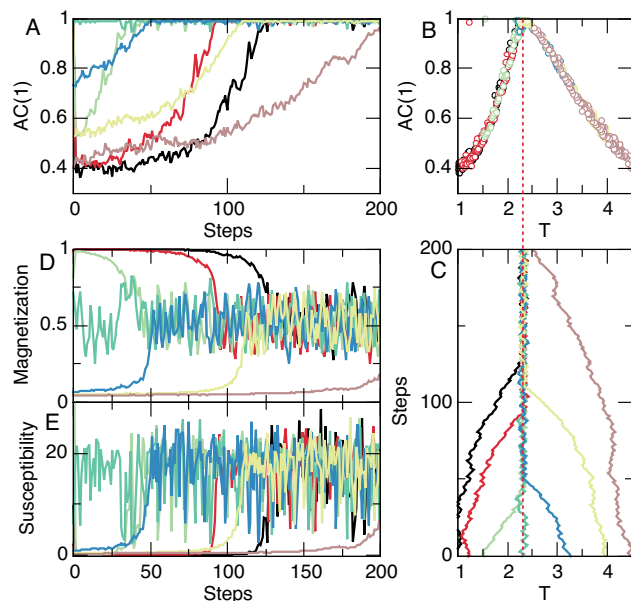


FIG. 2. Adaptive control of the Ising model with temperature adjusted iteratively by the autocorrelation of the order parameter. The data illustrate, for a variety of initial temperatures, the convergence of the system to the vicinity of the expected critical temperature $T_c = 2.3$. Panels A,C,D,E show, as a function of iteration steps, the first autocorrelation coefficient of the magnetization' fluctuations, the magnetization, the susceptibility, and the temperature. As seen in Panel C, for any initial temperature the system reaches a state fluctuating near the equilibrium T_c and at the maximum of $AC(1)$ (see panel A). Adaptation parameter $\kappa = 0.04$, other parameters as in Fig. 1.

To demonstrate control we proceed by choosing an initial random temperature and simulate the dynamics for some large number of Montecarlo (MC) steps, which we denote as an ‘‘adaptive iteration step’’ indexed by i . We proceed by estimating the $AC(1)$ of the fluctuations around the mean magnetization during the lapse of time corresponding to the adaptive iteration step i and monitor the change of $AC(1)$ between two consecutive steps i , defining

$$d_i = d_{i-1} \text{sign}[AC(1)_{(i)} - AC(1)_{(i-1)}], \quad (5)$$

so that d changes sign when a decrease in $AC(1)$ is de-

tected. We then use the gradient to its maximum value

$$\delta_i = (1 - AC(1)_{(i)})^2, \quad (6)$$

to change the future temperature $T(i+1)$ according to

$$T_{(i+1)} = T_{(i)} + \delta * d * \kappa, \quad (7)$$

where κ is a small constant that determines how slowly the temperature is adjusted. Its exact values is not crucial for the present results. Successive iterations of Eqs. 5–7 demonstrate convergence of the temperature to the expected value at equilibrium $T_c \sim 2.3$. Fig. 2 illustrates typical results for various initial temperatures, which in all cases converge to the vicinity of T_c . We note that the successive values of the parameters (order, control and $AC(1)$) obtained during the adaptive simulations over-imposes well (i.e., matches) those obtained from equilibrium simulations (i.e. the data of Fig. 1, see Suppl. Material).

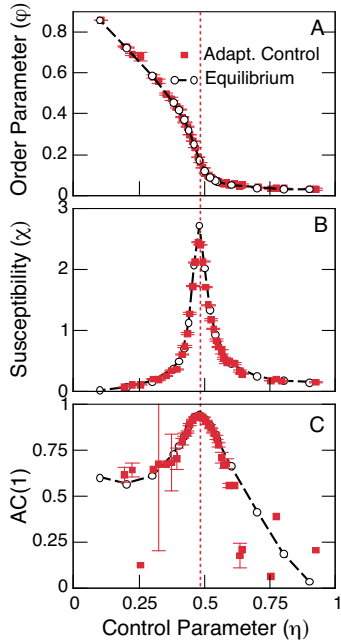


FIG. 3. 3D Vicsek model at equilibrium and under adaptive control. Order parameter φ (Panel A), the susceptibility χ (Panel B) (computed as $\text{var}(\varphi)/N$) and the first auto-correlation coefficient $AC(1)$ of the polarization fluctuations around the mean (Panel C) as function of η the control parameter. Notice the overlap between the equilibrium results (open circles) and the values reached during the adaptive control (filled squares) for different initial conditions which converge to the critical point denoted by the dashed line ($\eta_c \sim 0.48$). $N = 1024$, $v_0 = 1$, $\rho = 1.2$. $\kappa = 0.2$ and 10^3 MC steps per adaptive iteration step.

Vicsek model. We were also able to use the $AC(1)$ function to control the Vicsek model [12], the archetypal model for flocking behavior, towards its critical point. In this model, N self-propelled particles endowed with

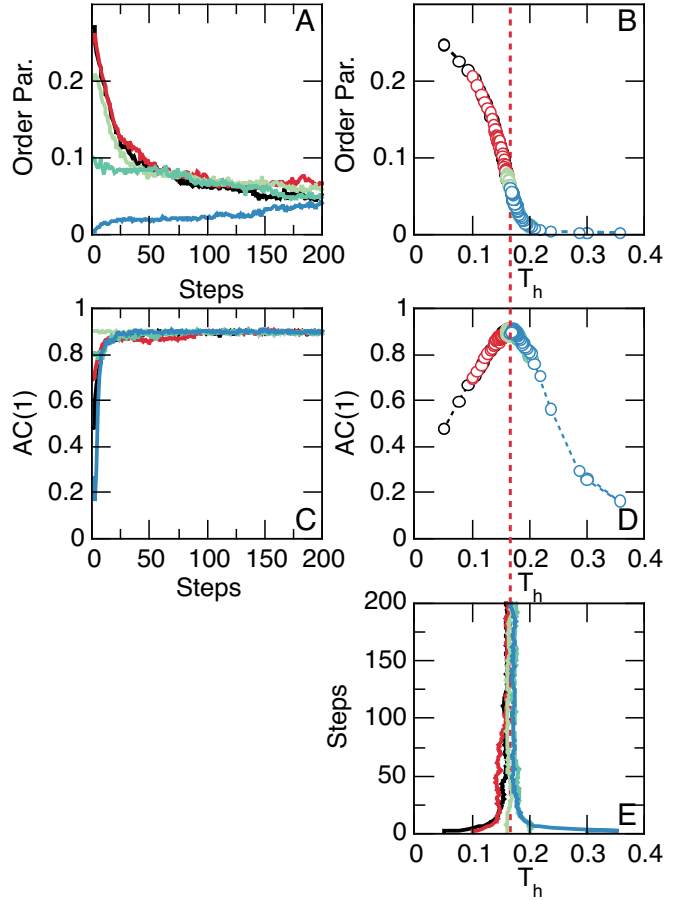


FIG. 4. Adaptive control of the neuronal network model. Data corresponds to numerical solutions of the model starting from five different initial conditions of the control parameter T_h . Nodes threshold T_h are adjusted iteratively according to Eqs. 5–7. Panels A, C and E show the evolution of the order parameter, $AC(1)$ and control parameter T_h respectively. These quantities are plotted against each other in Panels B and D to demonstrate convergence to the critical value of T_h (dashed red line) and to the maximum of $AC(1)$. $\kappa = 0.1$ and $5 * 10^3$ time steps per adaptive iteration step. Network parameters are: mean degree $\langle k \rangle = 10$, rewiring parameter $\beta = 0.3$, system size $N = 2^9$. Non null weights chosen from a distribution $p(w) = \lambda e^{-\lambda w}$ with $\lambda = 12.5$.

a fixed speed v_0 move in d -dimensional space. At each time step, positions $\mathbf{r}_i(t)$ and velocities $\mathbf{v}_i(t)$ are updated according to

$$\mathbf{v}_i(t + \Delta t) = v_0 \mathcal{R}_\eta \left[\sum_{j \in S_i} \mathbf{v}_j(t) \right], \quad (8)$$

$$\mathbf{r}_i(t + \Delta t) = \mathbf{r}_i(t) + \Delta t \mathbf{v}_i(t + \Delta t), \quad (9)$$

where S_i is a sphere of radius r_c centered at $\mathbf{r}_i(t)$. The operator \mathcal{R}_η normalizes its argument and rotates it randomly within a spherical cone centered at it and spanning a solid angle $\eta \Omega_d$, where Ω_d is the area of the unit

sphere in d dimensions ($\Omega_2 = 2\pi$, $\Omega_3 = 4\pi$).

The order parameter, which measures the degree of flocking, is the normalized modulus of the average velocity [12, 13],

$$\varphi \equiv \frac{1}{Nv_0} \left| \sum_{i=1}^N \mathbf{v}_i \right|. \quad (10)$$

$\varphi \in [0, 1]$, with $\varphi = O(1/\sqrt{N}) \sim 0$ in the disordered phase and $\varphi = O(1)$ in the ordered phase. We choose $\Delta t = r_c = 1$, so that the control parameters are the noise amplitude η , the speed v_0 and the number density $\rho = N/V$, where $V = L^d$ is the volume of the (periodic) box. We apply Eqs.5–7 to this model, using η as control parameter and keeping the density fixed. For comparison we over-plotted results from equilibrium runs with values taken during adaptive control of the simulations (Fig. 3). The close match demonstrates that the technique is able to control the flock model near its critical noise amplitude, $\eta_c \sim 0.48$ (see further details in Suppl. Material).

Neuronal network model. Successful control was further demonstrated for a neural network model [14] consisting of a network of interconnected nodes together with a dynamical rule. The model exhibits a second order phase transition [16] on a region of parameters. The model matrix of interactions follows a small-world topology and each node exhibits discrete state excitable dynamics, following the Greenberg-Hastings model [15]. Briefly, each node is assigned one of three states: quiescent Q , excited E , or refractory R , and the transition rules are: 1) $Q \rightarrow E$ with a small probability r_1 ($\sim 10^{-3}$), or if the sum of the connection weights w_{ij} with the active neighbors (j) is higher than a threshold T_h , i.e., $\sum w_{ij} > T_h$ and $Q \rightarrow Q$ otherwise; 2) $E \rightarrow R$ always; 3) $R \rightarrow Q$ with a small probability r_2 ($\sim 10^{-1}$) delaying the transition from the R to the Q state for some time steps. Parameters r_1 and r_2 , which determine the time scales of self-excitation and of recovery from the excited state, respectively, were kept fixed and T_h was updated according to control Eqs. (5–7). The density of active nodes, i.e. in state E , in each time step was taken as the order parameter. As shown for the previous models, $AC(1)$ was able to move and maintain the system near its critical point (here $T_h \sim 0.16$) (Fig. 4).

The present results applies, with some differences, to 1^{st} or 2^{nd} order phase transitions and also for low dimensional dynamical systems exhibiting continuous or discontinuous bifurcations from fixed points to limit cycles which can be controlled near the bifurcation point (see Suppl. Material).

In conclusion we have demonstrated, in three paradigmatic cases, how the autocorrelation function of the order parameter fluctuations allows to establish a feedback

loop for the control parameter to shift the system towards its critical point. Our results build on two previous lines of work which come close to describe the control strategy. One is the view of self-organized criticality [1] as a feedback between order and control parameters [17]. The other line relates to forecasting of an upcoming tipping point via the generic slowing down of criticality [18, 19]. The current results go beyond these previous approaches by demonstrating a mechanism that may explain the presence of criticality in some systems, and furthermore providing a strategy of control amenable of practical implementations in different areas. For instance, in neuroscience, this approach could be realized with optogenetical targeting [20] to clamp cortical networks to any desired dynamical state, helping to predict its influence on perceptual performance.

Acknowledgements. Supported by grant 1U19NS107464-01 from the NIH BRAIN Initiative (USA) and by CONICET (Argentina).

-
- [1] P. Bak, *How nature works: The science of self-organized criticality*. Springer Science, New York (1996).
 - [2] D.R. Chialvo, *Nature Physics* **6**, 744 (2010).
 - [3] T. Mora & W. Bialek, *J. Stat. Phys.* **144**, 268 (2011).
 - [4] A.R. Honerkamp-Smith, S.L. Veatch, S.L. Keller, *Biochim. Biophys. Acta* **1788**, 53 (2009).
 - [5] J.M. Beggs & D. Plenz, *Journal of Neuroscience* **23**, 11167 (2003).
 - [6] Q.Y. Tang, Y.Y. Zhang, J. Wang, W. Wang, D.R. Chialvo, *Phys. Rev. Lett.* **118**, 088102 (2017).
 - [7] A. Cavagna, I. Giardina, T.S. Grigera, *Physics Reports* **728**,1–62 (2018).
 - [8] M.A. Muñoz, *Rev. Mod. Phys.* **90**, 031001(2018).
 - [9] M.N. Barber, Finite-size scaling, in: C. Domb and J. L. Lebowitz (eds.), *Phase transitions and critical phenomena*, Academic Press, London (1983).
 - [10] A. Attanasi, et al. *Phys. Rev. Lett.* **113**, 238102 (2014).
 - [11] P.C. Hohenberg & B.I. Halperin, *Rev. Mod. Phys.* **49**, 435 (1977).
 - [12] T. Vicsek, et al. *Phys. Rev. Lett.* **75**, 1226 (1995).
 - [13] T. Vicsek & A. Zafeiris, *Physics Reports* **517**, 71 (2012).
 - [14] A. Haimovici, E. Tagliazucchi, P. Balenzuela, D.R. Chialvo, *Phys. Rev. Lett.* **110**, 178101 (2012).
 - [15] J.M. Greenberg & S.P. Hastings, *SIAM (Soc. Ind. Appl. Math.) J. Appl. Math.* **34**, 515, (1978).
 - [16] M. Zarepour, J.I. Perotti, O.V. Billoni, D.R. Chialvo S.A. Cannas. <https://arxiv.org/abs/1905.05280> (2019).
 - [17] D. Sornette, A. Johansen, I. Dornic, *J. Phys. I* **5**, 325–335 (1995).
 - [18] M. Scheffer, J. Bascompte, W.A. Brock, et al, *Nature* **461** 53–59 (2009).
 - [19] C. Boettiger, N. Ross, A. Hastings, *Theor Ecol* ; **6** 255–264 (2013).
 - [20] T. Bellay, A. Klaus, S. Seshadri, D. Plenz, *eLife* **4** e07224 (2015).